

Change in lumen eccentricity and asymmetry after treatment with Absorb bioresorbable vascular scaffolds in the ABSORB cohort B trial: a five-year serial optical coherence tomography imaging study



Pannipa Suwannasom^{1,2}, MD; Yohei Sotomi¹, MD; Taku Asano¹, MD; Jaryl Ng Chen Koon³, B.Eng; Hiroki Tateishi⁴, MD, PhD; Yaping Zeng⁴, MD, PhD; Erhan Tenekecioglu⁴, MD; Joanna J. Wykrzykowska¹, MD, PhD; Nicolas Foin³, PhD; Robbert J. de Winter¹, MD, PhD; John A. Ormiston⁵, MChB, PhD; Patrick W. Serruys^{6*}, MD, PhD; Yoshinobu Onuma^{4,7}, MD, PhD; on behalf of the investigators of the ABSORB Cohort B study

1. Academic Medical Center, Amsterdam, the Netherlands; 2. Heart Centre of Northern Thailand, Faculty of Medicine, Chiang Mai University, Chiang Mai, Thailand; 3. National Heart Centre Singapore, Singapore; 4. Thoraxcenter, Erasmus Medical Center, Rotterdam, the Netherlands; 5. Auckland City Hospital, Auckland, New Zealand; 6. International Centre for Circulatory Health, NHLI, Imperial College London, London, United Kingdom; 7. Cardialysis BV, Rotterdam, the Netherlands

GUEST EDITOR: Fernando Alfonso, MD; Hospital Universitario de La Princesa, Universidad Autónoma de Madrid, Madrid, Spain

KEYWORDS

- bioresorbable scaffold
- optical coherence tomography
- stable angina

Abstract

Aims: The aim of the study was to investigate long-term changes in lumen eccentricity and asymmetry at five years after implantation of the Absorb bioresorbable vascular scaffold (BVS).

Methods and results: Out of 101 patients from the ABSORB cohort B trial, 28 patients (29 lesions) with serial optical coherence tomography (OCT) examination at four different time points (cohort B1: post-procedure, six months, two, and five years [n=13]; cohort B2: post-procedure, one, three, and five years [n=16]) were evaluated. The longitudinal variance in lumen diameter was assessed by asymmetry index (AI). An asymmetric lesion was defined as AI >0.3. The circularity of the lumen or scaffold was evaluated by the eccentricity index calculated as minimal divided by maximal luminal or scaffold diameter per cross-section. The lowest lumen eccentricity index within a scaffold segment (EI_L) <0.7 was defined as an eccentric lesion. Post procedure, an eccentric lesion was observed in 72.4% and became concentric in 93.1% at five years (post EI_L 0.67±0.05 vs. five-year EI_L 0.80±0.10, p=0.03) with a modest reduction of the lumen area from baseline to five years by 0.75±0.32 mm². Asymmetric lumen morphology was observed in 93.1% (n=27) post implantation and persisted until five-year follow-up. On serial OCT analyses, there was a substantial increase in the scaffold EI during the first two years (post 0.70±0.06, six months 0.76±0.08, two years 0.85±0.07); then, it remained stable whereas the lumen circularity improved further. There were no significant differences in major adverse cardiac events regarding the lumen morphology over the five-year follow-up.

Conclusions: In patients treated with the Absorb BVS, the cross-sectional circularity improved over five years while the variance in longitudinal diameters remained. Regaining of lumen circularity is mainly caused by reshaping of the scaffold during the first two years.

*Corresponding author: Cardiovascular Science Division of the NHLI within Imperial College of Science, Technology and Medicine, South Kensington Campus, London, SW7 2AZ, United Kingdom. E-mail: patrick.w.j.c.serruys@pwserruys.com

Introduction

Bioresorbable vascular scaffold (BVS) technology has been developed to eliminate the deleterious caging effect of the permanent metallic stent. The mechanical behaviour of the BVS is different from metallic drug-eluting stents (DES). The BVS exhibits more lumen eccentricity and asymmetry than a metallic everolimus-eluting stent (EES) as assessed by intravascular ultrasound (IVUS) post implantation. The eccentricity and asymmetry of the device may cause an inhomogenous strut distribution, which theoretically may decrease local drug concentration¹ and alter shear stress, therefore promoting scaffold failure.

As demonstrated previously, the BVS struts gradually disappear over time. The initial eccentricity and asymmetry of the lumen may also change according to the full resorption of the struts and the remodelling of the vessel wall. Without the permanent metallic caging, the vessels may remodel and return to their original physiologic and morphologic state. Karanasos et al reported that, after full resorption of the first-generation BVS (ABSORB cohort A, n=4), the lumen asymmetry index decreased over time². However, the long-term lumen adaptation after second-generation BVS implantation has never been explored.

The aim of this study was to investigate, using optical coherence tomography (OCT), the eccentricity and asymmetry of the lumen at five years after implantation of the Absorb™ BVS (Abbott Vascular, Santa Clara, CA, USA) and their impact on long-term clinical outcomes.

Methods

STUDY DESIGN AND STUDY DEVICE

The ABSORB cohort B trial was a multicentre, prospective, open-label trial that included 101 patients (102 lesions) treated with the second-generation Absorb scaffold. The first 45 patients (cohort B1) underwent invasive coronary imaging at six-month, two-year, and five-year follow-up, while the other 56 patients (B2) underwent the same at one-, three-, and five-year follow-up. The long-term clinical outcomes were reported in all patients who had baseline OCT assessment. The clinical endpoint definitions have been published elsewhere³. The long-term changes of lumen morphology were exclusively reported only in lesions that had serial OCT assessment at all time points. The study protocol was approved by all institutional ethics committees and informed consent was obtained for every patient before any intervention was performed.

The Absorb BVS comprises a poly-L-lactide (PLLA) backbone coated with an amorphous drug-eluting coating matrix composed of poly-D,L-lactide (PDLLA) polymer containing everolimus 100 µg/cm². A pair of radiopaque platinum markers is located at the proximal and distal ends of the scaffold. Details of the study and treatment procedure have been described previously⁴.

IMAGING ACQUISITION AND ANALYSIS

OCT ACQUISITION

Over the last five years OCT techniques have evolved. OCT acquisition in this study was performed using four different

commercially available systems: the M2 and M3 time-domain systems and the C7 and C8 Fourier-domain systems (all LightLab Imaging; Westford, MA, USA). Details of the image acquisition have been described previously⁵.

OCT DATA ANALYSIS

The OCT images acquired post procedure and at follow-up were analysed off-line, using proprietary LightLab software (St. Jude Medical, St. Paul, MN, USA) and Q-Ivus 3.0 (Medis medical imaging systems, Leiden, the Netherlands). The scaffold segments and the 5 mm segments adjacent to both edges were analysed at 1 mm intervals by an independent core laboratory (Cardialysis, Rotterdam, the Netherlands).

OCT LUMEN ECCENTRICITY AND LUMEN ASYMMETRY

Lumen diameters in each cross-section were measured through each gravitational centre for each sectorial degree⁶. The variance in lumen diameter throughout the scaffold was assessed by an asymmetry index. The asymmetry index was calculated per scaffold segment as $(1 - [\text{minimal lumen diameter}/\text{maximal lumen diameter}])^7$. A lesion was characterised as an asymmetric lesion when the value of AI was over 0.3^{1,8,9}. Conversely, a lesion with an AI ≤ 0.3 was defined as a symmetric lesion.

The eccentricity index was calculated as a parameter for the circularity of cross-section using the formula of minimal luminal diameter divided by maximal luminal diameter from the same cross-section¹⁰. This parameter was calculated in all analysed frames and the most eccentric lumen shape in the scaffold segment was identified as the lowest value of eccentricity index (EI_L). A lesion with an $EI_L \geq 0.7$ was defined as concentric while an $EI_L < 0.7$ was defined as an eccentric lesion. The distinction between the method of calculation of eccentricity index and asymmetry index is illustrated and detailed in **Figure 1**.

The reference lumen area (RLA) was estimated as the mean lumen area between the 5 mm proximal and distal segments to the edges of the BVS⁸. Area stenosis (%) was calculated from $(1 - [\text{lumen area at the cross-section of interest}/\text{RLA}]) \times 100$.

CO-LOCALISATION OF POST-PROCEDURAL AND FOLLOW-UP OCT

Two post-procedural cross-sections were used as references to compare the changes of lumen area and the lumen eccentricity index at follow-up. The first cross-section was the site of post-procedural lowest eccentricity index (EI_L), while the second cross-section was the site of post-procedural highest eccentricity index (EI_H). The distance from the first cross-section comprising the distal marker to the EI_L or the EI_H cross-section was measured in the longitudinal view. Co-localisation of the corresponding cross-sections at all time points was performed by using the distance from the distal markers and topographical landmarks, such as side branch (SB), vein, pericardium, position and configuration of calcifications, in order to assure a precise co-localisation procedure. The serial changes of lumen area, lumen EI and neointimal thickness (reported as mean value of minimal, maximal and mean) in matched cross-sections were evaluated.

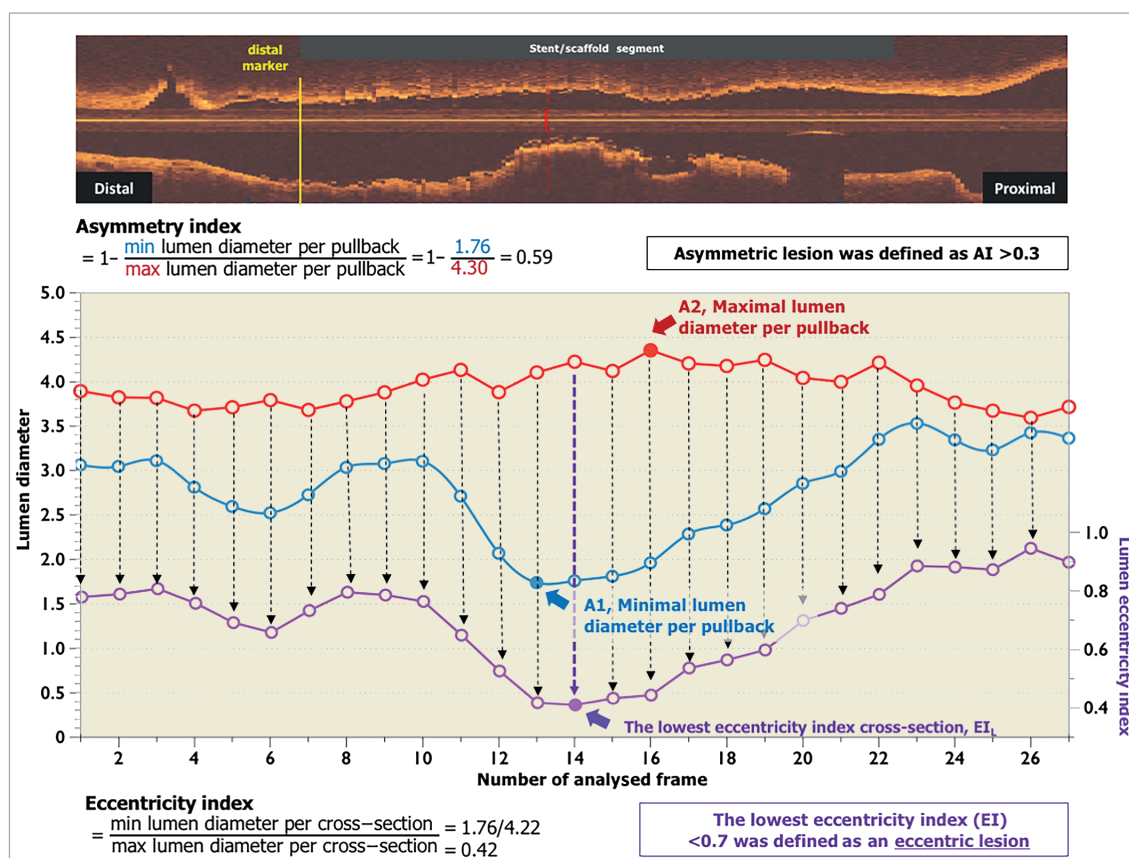


Figure 1. Differences between the methods used to calculate eccentricity index and asymmetry index. Asymmetry index was calculated per scaffold segment as $(1 - \text{minimal lumen diameter} / \text{maximal lumen diameter})$. Minimal lumen diameter was the minimal value of minimal lumen diameter throughout scaffold segment (A1), maximal lumen diameter was the maximal value of maximal lumen diameter throughout scaffold segment (A2). Therefore, the minimum lumen diameter and maximum lumen diameter could derive from different cross-sections in the scaffold segment. The eccentricity index used the formula of minimal lumen diameter divided by maximal lumen diameter in the same cross-section. This parameter was calculated in all analysed frames as shown by the individual purple dots. The most eccentric lumen shape in the scaffold segment was identified as the lowest value of eccentricity index. AI: asymmetry index; EI: eccentricity index

STATISTICAL ANALYSIS

All statistical analyses were performed using IBM SPSS Statistics, Version 23.0 (IBM Corp., Armonk, NY, USA). OCT analysis was performed per lesion. All continuous variables were presented as mean±standard deviation (SD) or median and interquartile range (IQR; 1st to 3rd quartile) as appropriate. Pairwise comparisons were performed by a Wilcoxon signed-rank test. All reported p-values were two-sided, and values of $p < 0.05$ were considered statistically significant.

Results

BASELINE CLINICAL AND ANGIOGRAPHIC CHARACTERISTICS, AND PROCEDURAL DETAILS

Out of 101 patients in the entire cohort, 28 patients (29 lesions) had serial OCT at all time points. Thirteen lesions from cohort B1 and 16 lesions from cohort B2 were included in the analysis, as shown in the flow chart (Figure 2). The patient, lesion and procedural characteristics are shown in Table 1. Post-dilation

was performed in 19 lesions (65.5%) with a maximal post-balloon dilation pressure of 17.79 ± 5.32 atm.

LUMEN MORPHOLOGY AT BASELINE

The baseline OCT results are detailed in Table 2. The post-procedural residual area stenosis was 1.0% (IQR -14.1%;13.2%) and the asymmetry index was 0.39 ± 0.06 . Out of 29 lesions, asymmetric morphology (AI > 0.3) was observed in 93.1% of lesions (n=27). The lumen EI_L was 0.67 ± 0.05 . Twenty-one lesions (72.4%) were classified as eccentric lesions. The highest eccentricity index (EI_H) was 0.92 ± 0.03 .

LUMEN MORPHOLOGY AT FIVE YEARS

Overall and individual changes in lumen morphology are presented in Figure 3. On average, both the asymmetry index and eccentricity index increased from post procedure to five years (asymmetry index: post 0.36 ± 0.05 vs. five-year 0.44 ± 0.11 , $p < 0.001$; eccentricity index: post 0.67 ± 0.05 vs. five-year 0.72 ± 0.09 , $p = 0.01$), indicating that the lumen became more concentric but longitudinally

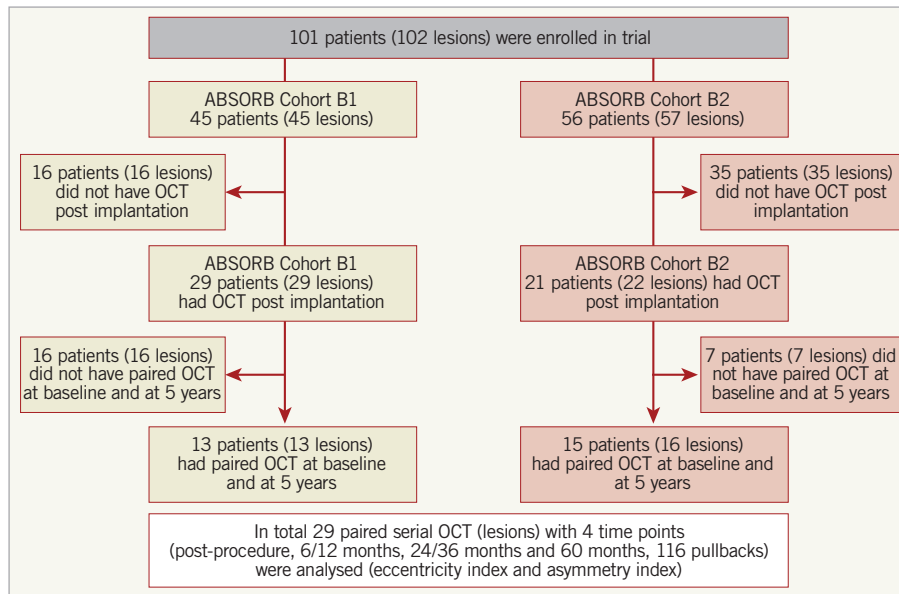


Figure 2. Study flow chart. OCT: optical coherence tomography

more asymmetric. The percentage of eccentric lesions decreased to 27.6%, whereas the proportion of asymmetric lesions remained unchanged (93.1%).

BASELINE LUMEN MORPHOLOGY AND THE LONG-TERM CLINICAL OUTCOMES

At baseline, there were 50 patients who had OCT assessment post procedure. The asymmetry index was 0.36 ± 0.07 and asymmetric

morphology (AI >0.3) was observed in 80% of lesions. The graphical presentation in **Figure 4** shows that major adverse cardiac events (MACE; a composite of cardiac death, all myocardial infarction and ischaemia-driven target lesion revascularisation) occurred in 10% of the asymmetric lesions and 10% of the symmetric lesions, $p=1.00$. Similarly, there were no significant differences in the eccentric lesions and concentric lesions (11.1% vs. 7.1%, $p=0.68$) over five-year follow-up.

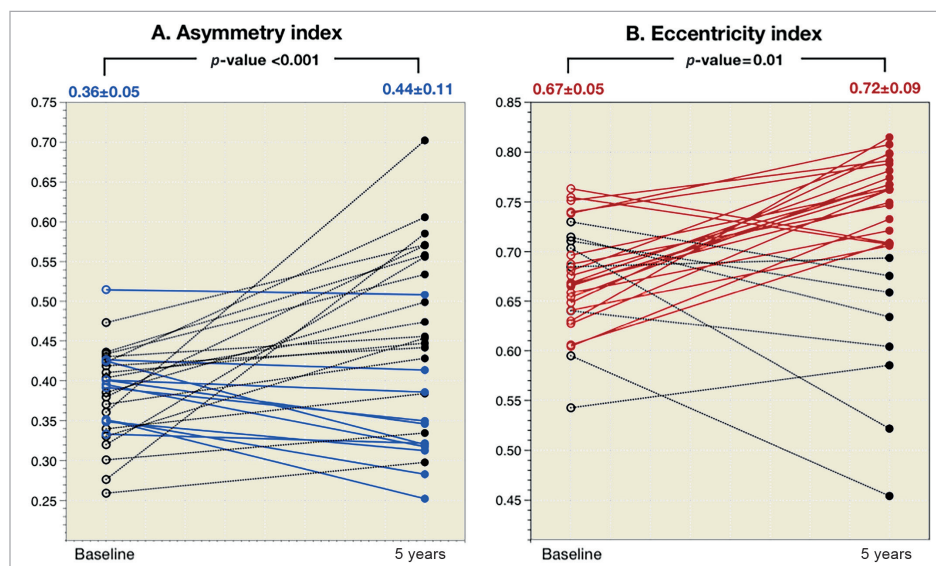


Figure 3. Individual asymmetry index and eccentricity index changes of the lumen between baseline and five years. A) Individual changes in the asymmetry index where blue lines connect individual cases in which the asymmetry index improves (lower than baseline); the dotted black lines connect the individual cases in which the asymmetry index becomes worse (higher than baseline). B) Individual changes in the eccentricity index where red lines connect individual cases in which the eccentricity index becomes concentric ($EI \geq 0.7$); the dotted black lines connect the individual cases in which it becomes eccentric ($EI < 0.7$). EI: eccentricity index

Table 1. Baseline patient and lesion characteristics, and procedural details.

		Overall N _p =28, N _L =29
Baseline patient characteristics		
Age, mean±SD		61.4±9.4
Male sex, n (%)		20 (71.4)
Hypertension, n (%)		17 (60.7)
Hyperlipidaemia, n (%)		24 (85.7)
Diabetes, n (%)		1 (3.6)
Current smoker, n (%)		10 (35.7)
Previous myocardial infarction, n (%)		9 (33.3)
Previous PCI, n (%)		7 (25.0)
Stable angina, n (%)		23 (82.1)
Baseline lesion characteristics		
Target vessel	Left anterior descending	15 (51.7)
	Left circumflex	6 (20.7)
	Right coronary artery	8 (27.6)
AHA/ACC lesion classification*	Type B1 lesion	20 (69.0)
	Type B2 lesion	8 (27.6)
Moderate/severe calcification		4 (13.3)
Procedural characteristics		
Predilatation performed, n (%)		29 (100)
Semi-compliant balloon used for predilatation		27 (93.1)
Maximal predilatation balloon diameter, mm		2.63±0.22
Length of predilatation balloon, mm		12.62±1.61
Maximal predilatation pressure, atm		12.00±3.14
Diameter of scaffold implanted, mm		3.0
Scaffold length, mm		18.0
Maximal device balloon inflation pressure, atm		13.17±2.90
Post-dilation balloon performed, n (%)		19 (65.5)
Maximal post-dilatation balloon diameter, mm		3.18±0.19
Maximal post-dilatation pressure, atm		17.79±5.32
Length of post-dilatation balloon, mm		11.70±3.13
Data are shown as mean±SD or median (IQR 1 st -3 rd) or n (%). *One piece of missing data in cohort B2. ACC: American College of Cardiology; AHA: American Heart Association; PCI: percutaneous coronary intervention		

SERIAL CHANGES OF LUMEN MORPHOLOGY UP TO FIVE YEARS

The changes in the eccentricity index at the site of the EI_L were assessed in matched cross-sections at all time points (Figure 5). The lumen EI_L increased substantially from baseline to two-year follow-up in parallel with the scaffold eccentricity index (Figure 5A). In the first two years after implantation, the improvement of lumen circularity was basically driven by reshaping of the scaffold. From one year to three years, the scaffold eccentricity index did not change, whereas the lumen circularity improved further (Figure 5B). In this period, the continuous growth of neointima contributed to the regaining of lumen circularity, which eventually

Table 2. OCT findings post-procedure and at 5-year follow-up.

	Post-procedure N=29	5 years N=29	p-value*
Reference lumen area, mm ²	6.22±1.68	5.83±1.51	0.19
Minimal lumen area, mm ²	5.96±0.93	3.84±1.35	<0.001
Mean lumen area, mm ²	7.40±1.05	5.98±1.30	<0.001
Minimal lumen diameter, mm	2.40±0.26	1.95±0.39	<0.001
Maximal lumen diameter, mm	3.72±0.26	3.53±0.45	<0.001
Minimal scaffold area, mm ²	6.19±0.93	n/a	
Mean scaffold area, mm ²	7.56±0.98	n/a	
Residual area stenosis (%)	1.0 (-14.1;13.2)	34.1 (18.5;45.3)	<0.001
Scaffold asymmetry index	0.36±0.05	0.44±0.11	<0.001
In-scaffold lowest lumen eccentricity index (EI _L)	0.67±0.05	0.72±0.09	0.01
In-scaffold highest lumen eccentricity index (EI _H)	0.92±0.03	0.94±0.02	0.002
Matched cross-section data at the site of the lowest eccentricity index post-procedure			
Lumen area at the site of EI _L , mm ²	6.83±1.37	6.09±1.69	0.049
Lumen eccentricity index	0.67±0.05	0.80±0.10	<0.001
Area stenosis at the site of EI _L (%)	-3.1 (-38.4;6.4)	-1.3 (-22.3;11.9)	0.11
Matched cross-section data at the site of the highest eccentricity index post-procedure			
Lumen area at the site of EI _H , mm ²	7.65±1.37	6.19±2.09	<0.001
Lumen eccentricity index	0.92±0.03	0.87±0.06	0.008
Area stenosis at the site of EI _H (%)	-26.7 (-48.4;-11.5)	-1.1 (-28.5;13.5)	0.004
Data are shown as mean±SD or median (IQR 1 st -3 rd) or n (%). The comparison was performed by Wilcoxon signed-rank test. *Comparison between baseline and 5 years. EI _L : post-procedural lowest eccentricity index per pullback; EI _H : post-procedural highest eccentricity index per pullback			

resulted in similar eccentricity of the lumen and scaffold at three years (Figure 5B). Serial changes of neointimal thickness at EI_L and EI_H cross-sections are tabulated in Table 3. The neointimal thickness of EI_H cross-sections was comparable to that of EI_L cross-sections.

At five-year follow-up, there was a substantial increase in the eccentricity index from baseline (0.67±0.05 to 0.80±0.10, p<0.001). The cross-section became more concentric in 82.8% with a modest reduction of the lumen area from baseline to five years by 0.75±0.32 mm². However, the reduction of lumen did not create a significant area stenosis at the site of EI_L (post-procedure -13.1% [IQR -38.4%;6.4%] vs. five years -1.3% [IQR -22.3%;11.9%], p=0.14).

Discussion

The main findings of the current analysis are the following: 1) the polymeric device has a high incidence of asymmetry (93.1%) and

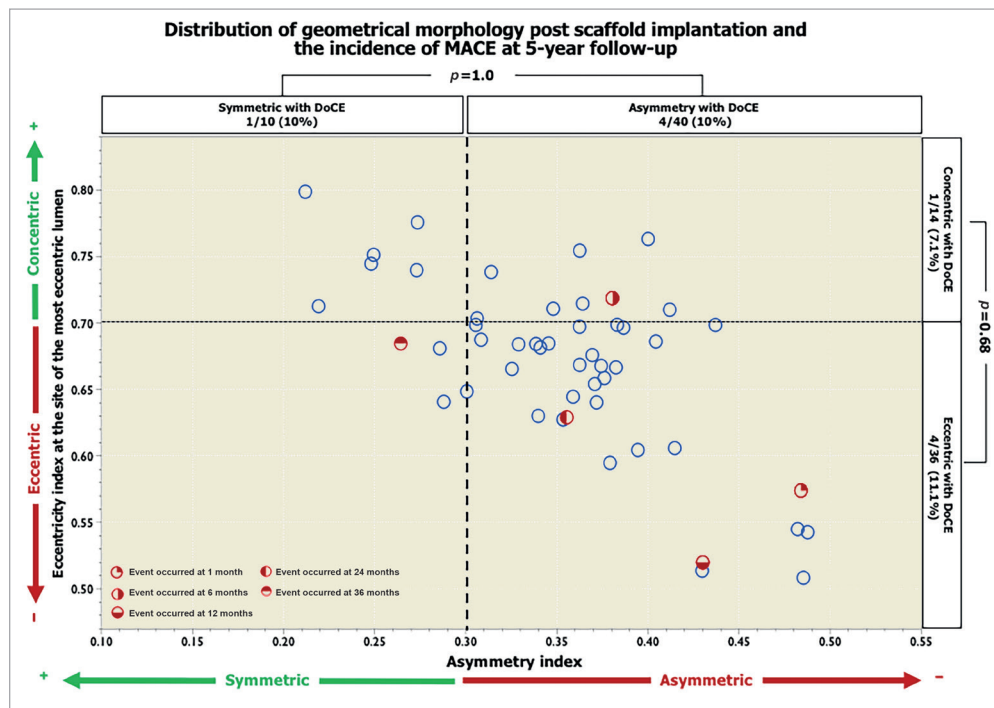


Figure 4. Distribution of geometrical morphology after scaffold implantation and the incidence of DoCE over five-year follow-up. The scatter plot represents the asymmetry index (AI) on the x-axis and the eccentricity index (EI) at the site of the most eccentric lumen on the y-axis. Red dots represent cases with major adverse cardiac events.

eccentricity (72.4%) of the lumen post implantation; 2) at five-year follow-up, the lumen shape of the scaffold segment became more circular; 3) the lumen asymmetry did not improve in the long-term follow-up, suggesting that longitudinal heterogeneity of the lumen diameters persisted.

Recently, the prospective randomised controlled ABSORB II trial comparing the Absorb BVS and the XIENCE stent (Abbott Vascular) reported that high AI (>0.3) was associated with an increase in the device-oriented composite endpoint (DoCE), mainly driven by myocardial infarction¹¹, suggesting that the

Table 3. Comparison of neointimal thickness between the lowest eccentricity index cross-section and the highest eccentricity index cross-section.

Matched cross-section data	6 months (N=13, L=13)	1 year (N=15, L=16)	2 years (N=13, L=13)	3 years (N=15, L=16)
At the site of the lowest eccentricity index post-procedure (EI_L)				
Minimal neointimal thickness at the site of EI _L [*] , μm	15.8±18.3	72.5±69.9	113.8±66.2	105.0±61.5
Maximal neointimal thickness at the site of EI _L [*] , μm	460.8±340.8	400.6±140.3	466.2±150.6	412.5±97.6
Mean neointimal thickness at the site of EI _L , μm	204.2±75.7	207.5±81.3	286.2±79.1	261.9±73.4
At the site of the highest eccentricity index post-procedure (EI_H)				
Minimal neointimal thickness at the site of EI _H [*] , μm	95.4±75.9	71.9±64.0	129.2±74.9	127.5±67.1
Maximal neointimal thickness at the site of EI _H [*] , μm	340.8±130.4	363.1±216.6	403.9±140.2	370.6±139.5
Mean neointimal thickness at the site of EI _H , μm	216.9±89.5	196.3±75.5	253.9±78.5	240.0±74.1
Comparison of neointimal thickness				
p-value for minimal neointimal thickness [#]	0.007	0.08	0.58	0.30
p-value for maximal neointimal thickness ^{**}	0.18	0.55	0.19	0.33
p-value for mean neointimal thickness [†]	0.79	0.56	0.21	0.27
Data are shown as mean±SD or median (IQR 1 st -3 rd) or n (%). [*] represents mean value; [#] comparison between minimal neointimal thickness of EI _L and EI _H ; ^{**} comparison between maximal neointimal thickness of EI _L and EI _H ; [†] comparison between mean neointimal thickness of EI _L and EI _H ; EI _H : post-procedural highest eccentricity index value in scaffold segment; EI _L : post-procedural lowest eccentricity index value in scaffold segment				

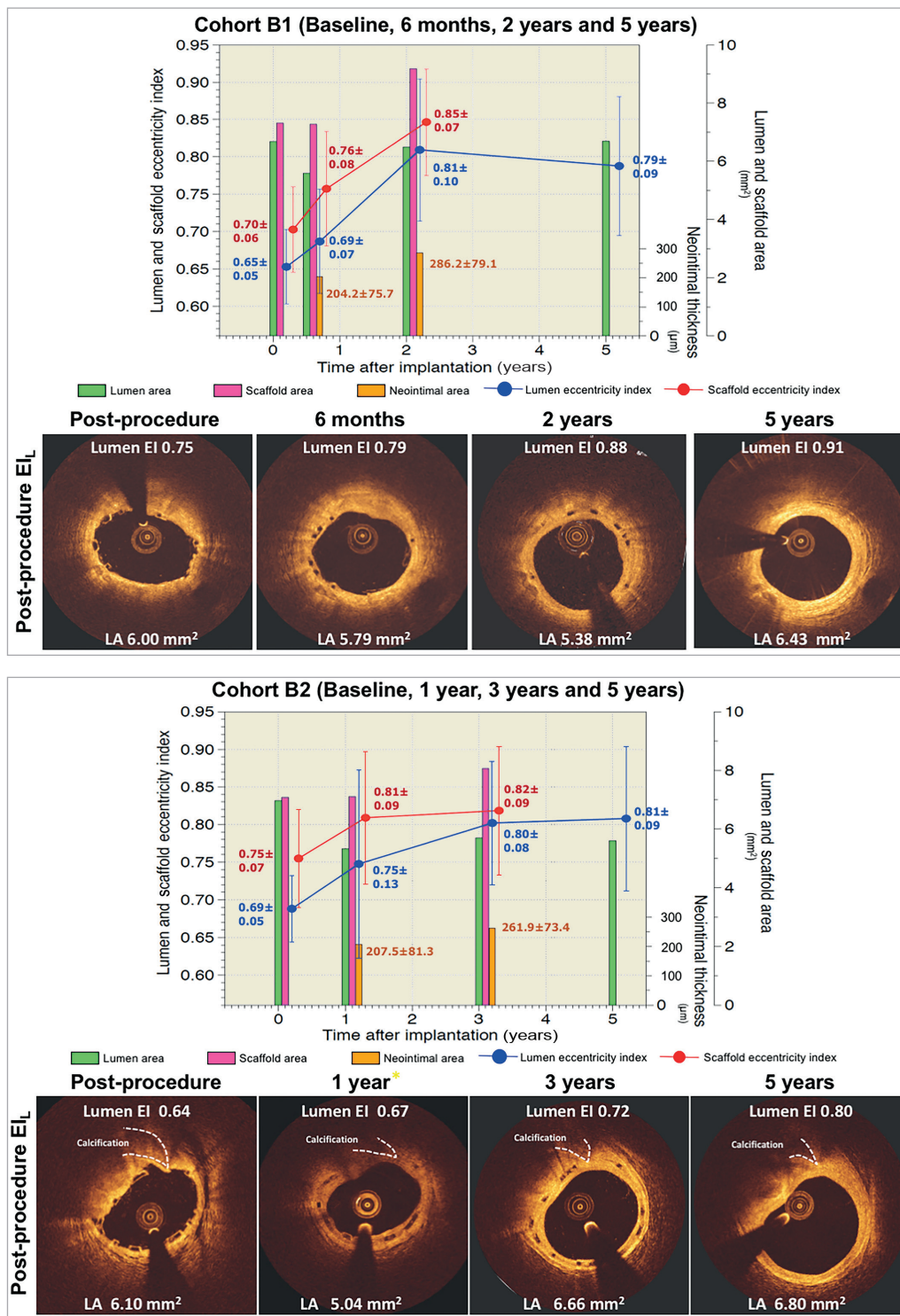


Figure 5. Serial changes of lumen and scaffold area and lumen and scaffold eccentricity index of matched cross-sections at the site of the lowest value of the post-procedural eccentricity index in cohort B1 and cohort B2. The bar graphs in green and magenta colours represent lumen area and scaffold area, respectively. The bar graphs in orange represent the neointimal thickness in micrometres. The blue circles and vertical lines represent the mean and standard error of the mean of EI_L post procedure, whereas the red circles and vertical lines represent the mean and standard error of the mean of the scaffold eccentricity index at the same cross-section. The EI_L substantially increased from baseline to two-year follow-up (blue line, panel A), in parallel with the scaffold eccentricity index (red line, panel A). In the first two years after implantation, the improvement of lumen circularity is basically driven by the reshaping of the scaffold area. From one year to three years, the eccentricity of the scaffold did not change, whereas the lumen circularity improved further (blue line, panel B). The continuous growth of neointimal tissue also contributed to the regaining of lumen circularity and eventually resulted in similar eccentricity of the lumen and scaffold area at three years (bar graph in orange colour).

heterogeneity in lumen diameters and lumen areas throughout the scaffold could have pathophysiologic implications in early and medium-term follow-up. However, the current analysis showed that the asymmetric lesions as well as eccentric lesions were not associated with MACE at five-year follow-up. The discrepancy of the results might be explained by the small sample size and low event rates in the trial.

In previous studies where IVUS and OCT were used, both modalities showed that the eccentricity did not affect neointimal growth^{12,13}. The current analysis showed similar findings: the neointimal thickness between the EI_L and EI_H cross-sections was comparable.

PRACTICAL IMPLICATIONS

Recent IVUS studies have demonstrated that post-procedural asymmetry of a stent or scaffold is an independent determinant of device-oriented clinical events (DoCE), irrespective of the expansion index¹¹. However, attempting to correct the eccentricity and asymmetry of the lumen may be troublesome. Both aggressive predilation and aggressive post-dilation may correct the lumen eccentricity (calculated in one cross-section); on the other hand, they may not be able to change the gap between minimal and maximal lumen diameters, due to the fact that the balloon also increases the lumen diameters in both cross-sections (**Figure 1**). Systematic aggressive lesion preparation with a non-compliant balloon in combination with routine high-pressure post-dilation (with a non-compliant balloon), as previously reported by Mattasini et al¹⁴, would be the strategy of choice to avoid the eccentric and asymmetric lumen morphology.

So far, evidence of eccentric and asymmetric lumen morphology post implantation and of clinical outcomes is sparse. Online OCT guidance during the procedure to correct asymmetric and eccentric lumen morphology with shear stress analysis would be of interest in further clinical trials.

Limitations

There are several limitations in the present study that should be acknowledged. First, the analysis was based solely on the cases that had serial OCT at all time points; therefore, it was inevitable to have a small sample size with potential selection bias. The findings should be interpreted with caution as the ABSORB cohort B included relatively simple lesion characteristics. The results of the present study may not be applicable in complex lesions. In addition, the data were derived from subgroup analysis; therefore, the study is hypothesis-generating in nature. Second, pre-procedure OCT images were not available; pre-existing asymmetric or eccentric lesions certainly affect the scaffold morphology after deployment. Third, the software and catheters differed throughout the study period because of advances in technology. However, both eccentricity and asymmetry indices were calculated by using the ratio of lumen diameters; thus, the values would not be influenced by the different types of OCT system. Fourth, because of the limited penetration

of OCT, the present analysis was unable to assess whether there was a relationship between the lumen morphological changes and plaque burden, plaque progression or regression, alteration of plaque type and vessel remodelling. To address the questions raised above, co-localisation of OCT and IVUS images is a prerequisite. Further analyses of plaque composition, vascular remodelling and wall shear stress profiling as assessed by IVUS may provide more mechanistic details of luminal change over time.

Conclusions

In patients treated with Absorb bioresorbable scaffolds, the cross-sectional circularity improved over five years while the variance in longitudinal diameters remained without creating a significant stenosis. Regaining of lumen circularity is mainly caused by reshaping of the scaffold during the first two years.

Impact on daily practice

The polymeric device has a high incidence of asymmetry and eccentricity of the lumen post implantation. Previous IVUS data have shown that a post-procedural asymmetric lesion is associated with one-year clinical events, mainly driven by MI. The present study demonstrated that, at five-year follow-up, the lumen could regain its circularity but the asymmetry of the lumen still persisted. Asymmetric lesions were not associated with MACE at five-year follow-up, albeit in a limited sample size. The strategies to avoid eccentricity and asymmetry of the lumen post implantation remain challenging and need further investigation.

Guest Editor

This paper was guest edited by Fernando Alfonso, MD; Hospital Universitario de La Princesa, Universidad Autónoma de Madrid, Madrid, Spain.

Funding

The ABSORB cohort B trial was sponsored by Abbott Vascular. ClinicalTrials.gov Identifier: NCT00856856.

Conflict of interest statement

P. Serruys and Y. Onuma are members of the international advisory board of Abbott Vascular. The other authors have no conflicts of interest to declare. The Guest Editor has no conflicts of interest to declare.

References

1. Brugaletta S, Gomez-Lara J, Diletti R, Farooq V, van Geuns RJ, de Bruyne B, Dudek D, Garcia-Garcia HM, Ormiston JA, Serruys PW. Comparison of in vivo eccentricity and symmetry indices between metallic stents and bioresorbable vascular scaffolds: insights from the ABSORB and SPIRIT trials. *Catheter Cardiovasc Interv.* 2012;79:219-28.

2. Hwang CW, Wu D, Edelman ER. Physiological transport forces govern drug distribution for stent-based delivery. *Circulation*. 2001;104:600-5.
3. Karanasos A, Simsek C, Gnanadesigan M, van Ditzhuijzen NS, Freire R, Dijkstra J, Tu S, Van Mieghem N, van Soest G, de Jaegere P, Serruys PW, Zijlstra F, van Geuns RJ, Regar E. OCT assessment of the long-term vascular healing response 5 years after everolimus-eluting bioresorbable vascular scaffold. *J Am Coll Cardiol*. 2014;64:2343-56.
4. Serruys PW, Ormiston J, van Geuns RJ, de Bruyne B, Dudek D, Christiansen E, Chevalier B, Smits P, McClean D, Koolen J, Windecker S, Whitbourn R, Meredith I, Wasungu L, Ediebah D, Veldhof S, Onuma Y. A Polylactide Bioresorbable Scaffold Eluting Everolimus for Treatment of Coronary Stenosis: 5-Year Follow-Up. *J Am Coll Cardiol*. 2016;67:766-76.
5. Tateishi H, Suwannasom P, Sotomi Y, Nakatani S, Ishibashi Y, Tenekecioglu E, Abdelghani M, Cavalcante R, Zeng Y, Grundeken MJ, Albuquerque FN, Veldhof S, Onuma Y, Serruys PW; investigators of the ABSORB Cohort B study. Edge Vascular Response After Resorption of the Everolimus-Eluting Bioresorbable Vascular Scaffold - A 5-Year Serial Optical Coherence Tomography Study. *Circ J*. 2016;80:1131-41.
6. Gogas BD, Serruys PW, Diletti R, Farooq V, Brugaletta S, Radu MD, Heo JH, Onuma Y, van Geuns RJ, Regar E, De Bruyne B, Chevalier B, Thuesen L, Smits PC, Dudek D, Koolen J, Windecker S, Whitbourn R, Miquel-Hebert K, Dorange C, Rapoza R, Garcia-Garcia HM, McClean D, Ormiston JA. Vascular response of the segments adjacent to the proximal and distal edges of the ABSORB everolimus-eluting bioresorbable vascular scaffold: 6-month and 1-year follow-up assessment: a virtual histology intravascular ultrasound study from the first-in-man ABSORB cohort B trial. *JACC Cardiovasc Interv*. 2012;5:656-65.
7. Tsuchida K, Garcia-Garcia HM, Ong AT, Valgimigli M, Aoki J, Rademaker TA, Morel MA, van Es GA, Bruining N, Serruys PW. Revisiting late loss and neointimal volumetric measurements in a drug-eluting stent trial: analysis from the SPIRIT FIRST trial. *Catheter Cardiovasc Interv*. 2006;67:188-97.
8. de Jaegere P, Mudra H, Figulla H, Almagor Y, Doucet S, Penn I, Colombo A, Hamm C, Bartorelli A, Rothman M, Nobuyoshi M, Yamaguchi T, Voudris V, DiMario C, Makovski S, Hausmann D, Rowe S, Rabinovich S, Sunamura M, van Es GA. Intravascular ultrasound-guided optimized stent deployment. Immediate and 6 months clinical and angiographic results from the Multicenter Ultrasound Stenting in Coronaries Study (MUSIC Study). *Eur Heart J*. 1998;19:1214-23.
9. Mintz GS, Nissen SE, Anderson WD, Bailey SR, Erbel R, Fitzgerald PJ, Pinto FJ, Rosenfield K, Siegel RJ, Tuzcu EM, Yock PG. American College of Cardiology Clinical Expert Consensus Document on Standards for Acquisition, Measurement and Reporting of Intravascular Ultrasound Studies (IVUS). A report of the American College of Cardiology Task Force on Clinical Expert Consensus Documents. *J Am Coll Cardiol*. 2001;37:1478-92.
10. von Birgelen C, Gil R, Ruygrok P, Prati F, Di Mario C, van der Giessen WJ, de Feyter PJ, Serruys PW. Optimized expansion of the Wallstent compared with the Palmaz-Schatz stent: on-line observations with two- and three-dimensional intracoronary ultrasound after angiographic guidance. *Am Heart J*. 1996;131:1067-75.
11. Suwannasom P, Sotomi Y, Ishibashi Y, Cavalcante R, Albuquerque FN, Macaya C, Ormiston JA, Hill J, Lang IM, Eged M, Fajadet J, Lesiak M, Tijssen JG, Wykrzykowska JJ, de Winter RJ, Chevalier B, Serruys PW, Onuma Y. The Impact of Post-Procedural Asymmetry, Expansion, and Eccentricity of Bioresorbable Everolimus-Eluting Scaffold and Metallic Everolimus-Eluting Stent on Clinical Outcomes in the ABSORB II Trial. *JACC Cardiovasc Interv*. 2016;9:1231-42.
12. Kim BK, Ko YG, Oh S, Kim JS, Kang WC, Jeon DW, Yang JY, Choi D, Hong MK, Ahn T, Jang Y. Comparisons of the effects of stent eccentricity on the neointimal hyperplasia between sirolimus-eluting stent versus paclitaxel-eluting stent. *Yonsei Med J*. 2010;51:823-31.
13. Kaneda H, Ako J, Honda Y, Terashima M, Morino Y, Yock PG, Popma JJ, Leon MB, Moses JW, Fitzgerald PJ. Impact of asymmetric stent expansion on neointimal hyperplasia following sirolimus-eluting stent implantation. *Am J Cardiol*. 2005;96:1404-7.
14. Mattesini A, Secco GG, Dall'Ara G, Ghione M, Rama-Merchan JC, Lupi A, Viceconte N, Lindsay AC, De Silva R, Foin N, Naganuma T, Valente S, Colombo A, Di Mario C. ABSORB biodegradable stents versus second-generation metal stents: a comparison study of 100 complex lesions treated under OCT guidance. *JACC Cardiovasc Interv*. 2014;7:741-50.